optica

Single-shot carrier-envelope-phase measurement in ambient air: supplementary material

M. Kubullek[1], Z. Wang[1,2], K. von der Brelje[1], D. Zimin[1,2], P. Rosenberger[1], J. Schötz[1,2], M. Neuhaus[1], S. Sederberg[3], A. Staudte[3], N. Karpowicz[2], M. F. Kling[1,2], and B. Bergues[1,2,3,*]

[1]Physics Department, Ludwig-Maximilians-Universität Munich, Am Coulombwall 1, 85748 Garching, Germany
[2]Max-Plack-Institut für Quantenoptik, Hans-Kopfermann-Straße 1, 85748 Garching, Germany
[3]Joint Attosecond Science Laboratory, National Research Council of Canada and University of Ottawa, Ottawa, Ontario K1A0R6, Canada
*Corresponding author: boris.bergues@mpq.mpg.de

Published 7 January 2020

This document provides supporting information for "Single-shot carrier-envelope-phase measurement in ambient air," https://doi.org/10.1364/OPTICA.7.000035. We include details about the experimental setup and beam diagnostics as well as additional measurement data.

EXPERIMENTAL SETUP

The experimental setup is shown in Fig. S2. The laser pulses for the experiment are obtained from a 10 kHz Ti:Sapphire chirped pulse amplification system (Femtopower HR, Spectra Physics). The linearly polarized output pulses with a central wavelength of 780 nm are spectrally broadened in an argon gas-filled hollow core fiber and subsequently compressed to sub 4 fs duration with a set of chirped mirrors. The laser intensity is adjusted in the experiment using a filter wheel. A pair of wedges is used to optimize the dispersion, and to vary the glass thickness in dispersion scan measurements. A broadband $\lambda/4$-waveplate is used to generate circular polarized pulses. The beam is then focused in ambient air between the electrodes of the phase meter using an $f = 350$ mm spherical focusing mirror. The sample is mounted on a manual xyz-micrometer stage. The focal plane is imaged using a CMOS camera placed behind the sample.

The photocurrent signal is preamplified using two variable gain current-to-voltage transimpendance amplifiers (DLPCA-200, FEMTO), and integrated with two gated boxcar integrators (SR250, Stanford Research Systems) triggered at the laser repetition rate. The integrated signal is then recorded using a DAQ-card and saved for further processing and analysis.

SAMPLE MICROSCOPE IMAGE

An optical microscope image of the phase-meter electrodes is shown in Fig. S1. The copper electrodes are 1 mm thick and are typically 60 to 90 µm appart.

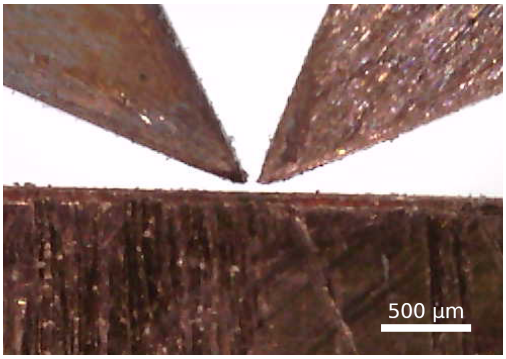

Fig. S1. Optical microscope image of the copper electrodes.

LASER SPECTRUM

The spectrum of the input laser pulses is shown in Fig S3. Its bandwidth supports a Fourier limited pulse with a duration Δt ~3.5 fs FWHM (full-width-at-half-maximum) of the intensity profile.

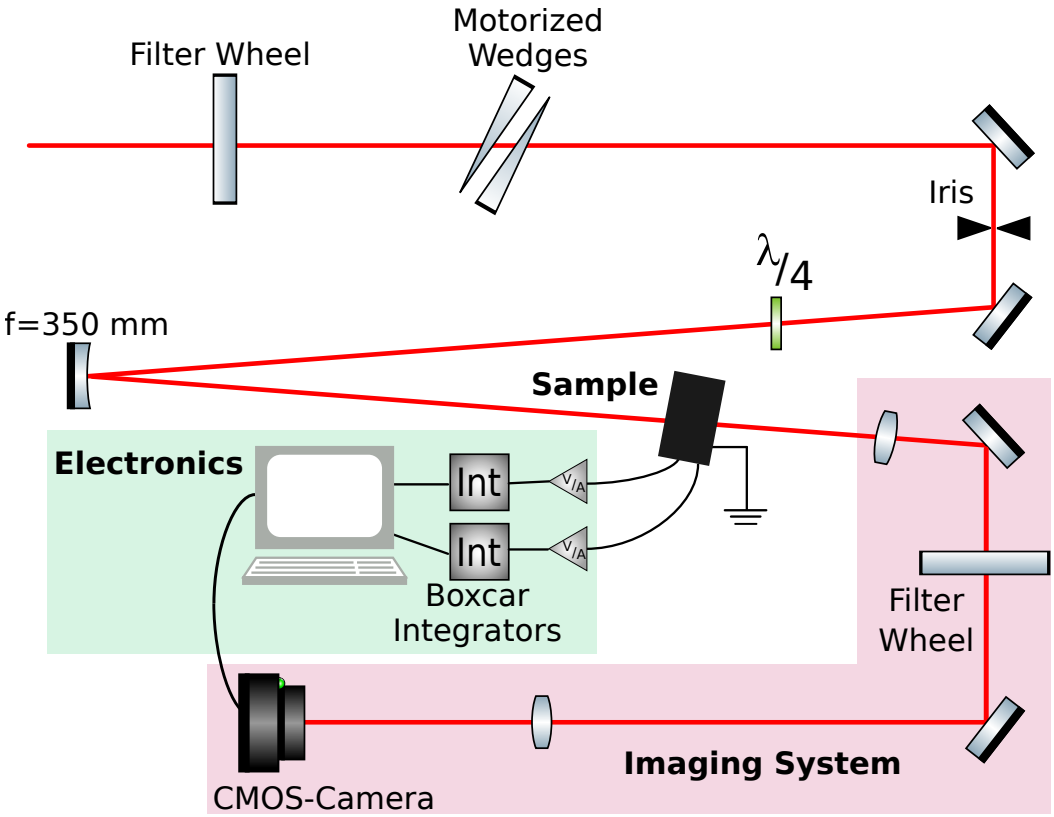

Fig. S2. Schematic view of the setup used for the CP-phase-meter mesurements in ambient air.

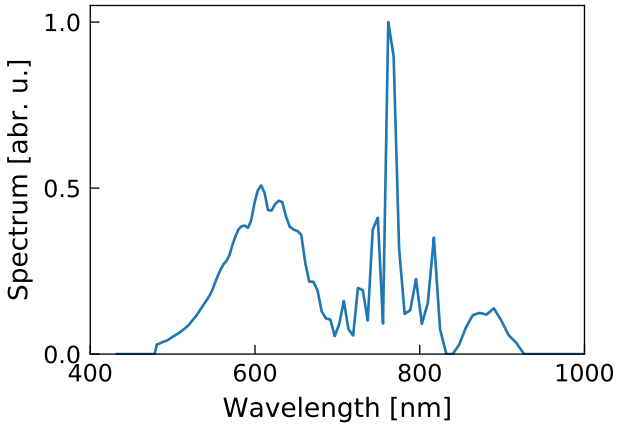

Fig. S3. Typical spectrum of the few-cycle pulses used in the experiment.

MEASUREMENT OF THE PEAK INTENSITY

We describe the intensity profile of the laser pulses at the focus with a Gaussian shaped profile in time and space:

$$I(x,y,t) = I_0\, e^{-4\ln 2\left(\frac{x}{\Delta x}\right)^2} e^{-4\ln 2\left(\frac{y}{\Delta y}\right)^2} e^{-4\ln 2\left(\frac{t}{\Delta t}\right)^2} \quad \text{(S1)}$$

where I_0 is the peak intensity, and Δx, Δy and Δt are the FWHM of the pulses in the spatial and temporal domain. The peak intensity I_0 is calculated from the average optical power P_{avg} and the repetition rate of the laser system f_{rep}:

$$I_0 = \left(\frac{4\ln 2}{\pi}\right)^{3/2} \frac{P_{\text{avg}}}{f_{\text{rep}}\,\Delta t\,\Delta x\,\Delta y} \quad \text{(S2)}$$

The image of the laser focus is shown in Fig. S4. Fitting the recorded intensity map with a two-dimensional Gaussian function results in $\Delta x = 33.6\,\mu\text{m}$ and $\Delta y = 31.5\,\mu\text{m}$. With a typical laser pulse duration of $\Delta t = 4\,\text{fs}$ and an average optical power of $P_{\text{avg}} = 980\,\text{mW}$ we obtain a peak intensity of $I_0 = 2\times 10^{15}\,\text{W cm}^{-2}$.

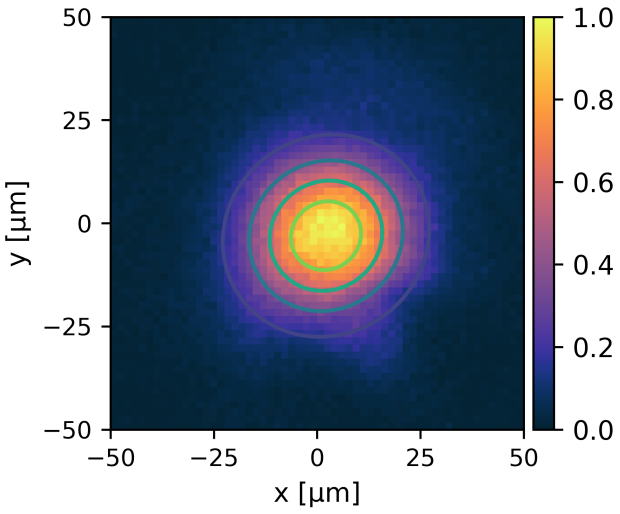

Fig. S4. Image of the laser focus. The contour lines represent the shape of the fitted two-dimensional Gaussian function.

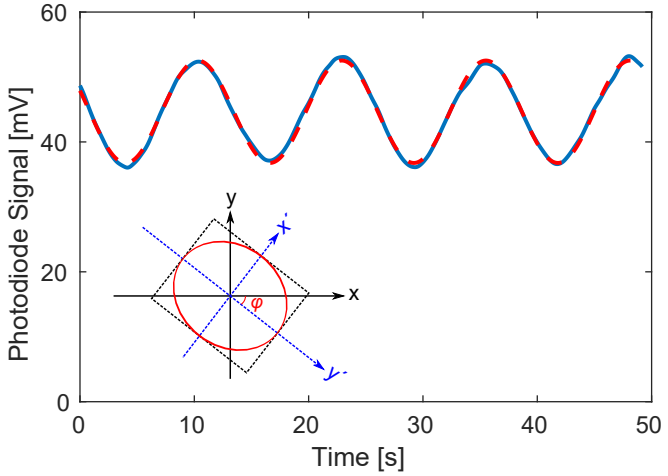

Fig. S5. Measured (solid blue) and fitted (dashed red) polarization curve by recording the photodiode signal after a continuously rotating linear polarizer. Inset: the schematics of laser polarization with ellipticity $\varepsilon = 0.84$ and orientation angle $\varphi = 38°$

MEASUREMENT OF THE ELLIPTICITY

The polarization of an elliptically polarized electric field is described by

$$\mathbf{E}(t,\mathbf{r}) = \frac{E_0}{\sqrt{1+\varepsilon^2}} \begin{pmatrix} \cos(\omega_0 t + \phi_{CE}) \\ \varepsilon \sin(\omega_0 t + \phi_{CE}) \\ 0 \end{pmatrix}, \qquad \text{(S3)}$$

where ω_0 is the angular frequency, ε the ellipticity, and ϕ_{CE} the CEP.

In order to measure the ellipticity, the laser pulses are sent through a continuously rotating linear polarizer, while the transmitted power is recorded with a photodiode. The results are shown in Fig. S5. The transmitted power P_t for a polarizer angle θ is described by:

$$P_t \propto \frac{\cos^2(\theta) + \varepsilon^2 \sin^2(\theta)}{1+\varepsilon^2}. \qquad \text{(S4)}$$

The measured data presented in Fig. S5 is fitted using Eq. S4, yielding an ellipticity of $\varepsilon = 0.84$. The orientation angle $\varphi = 38°$ of the polarization ellipse is shown in the inset of Fig. S5. Thus, the few-cycle pulses used in our experiments are close to, although not perfectly, circularly polarized.

CEP-TAGGING ON LONGER TIME SCALES

In Fig. S6 we show the parametric plot obtained from the one minute long measurement discussed in the main text. Following the procedure described in there, we determine an upper limit of 356 mrad for the uncertainty of this measurement, which includes 600 000 laser shots.

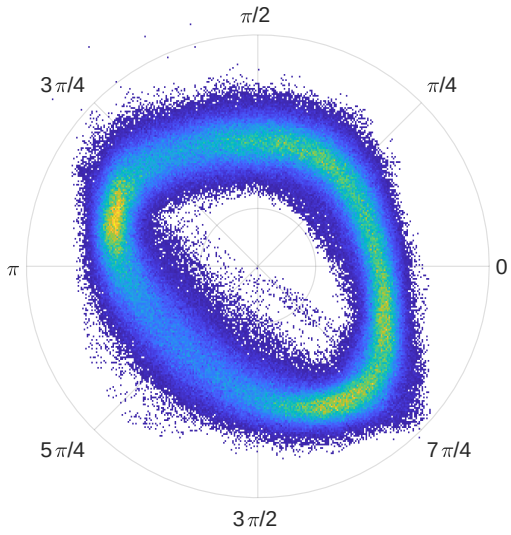

Fig. S6. Parametric plot corresponding to an acquisition time of one minute.

SENSITIVITY OF THE MEASUREMENT AS A FUNCTION OF PULSE COMPRESSION

In Fig. 3 of the main manuscript, we present the single-shot current signals recorded while linearly changing the amount of dispersive material in the beam path. In order to discuss the sensitivity of the measurement as a function of pulse compression, we present in Fig. S7 the parametric

plots corresponding to selected regions of the dispersion scan. The data processing, i.e. the recentering and normalization procedure is the same as outlined in the main article.

For each region, the uncertainty of the CEP-measurement is calculated as described in the main article from the relative radial error dr/r of the parametric plot. The results are summarized in table S1.

Parametric Plot	CEP uncertainty
(a)	134 mrad
(b)	160 mrad
(c)	188 mrad
(d)	243 mrad

Table S1. Uncertainties of the CEP measurement for different pulse compressions.

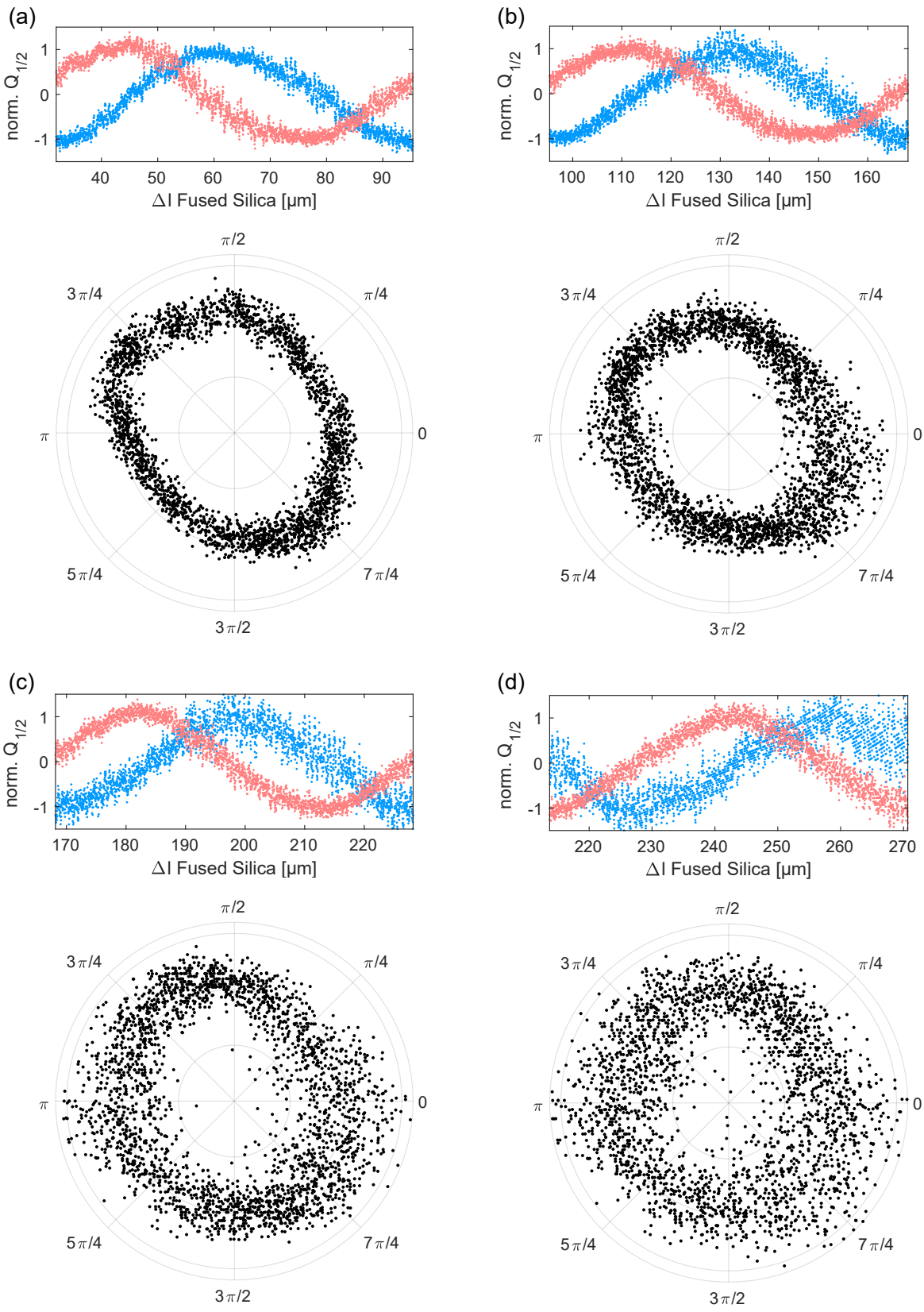

Fig. S7. Normalized single-shot current signals and corresponding parametric plots for different parts of the dispersion scan presented in the main text. (a) 35 µm to 95 µm, (b) 95 µm to 165 µm, (c) 170 µm to 230 µm, (d) 215 µm to 270 µm fused silica.